Corrections for effects of biaxial stresses in annealed glass

Ilham Nurhuda[*1,2], Nelson T.K. Lam[1], Emad F. Gad[1,3] and Ignatius Calderone[4]

[1]*Department of Civil and Environmental Engineering, The University of Melbourne, Australia*
[2]*Department of Civil Engineering, Universitas Diponegoro, Semarang, Indonesia*
[3]*Faculty of Engineering & Industrial Sciences, Swinburne University of Technology, Australia*
[4]*Calderone and Associates Pty Ltd. Consulting Engineers, Australia*

Abstract. Experimental tests have shown that glass exhibits very different strengths when tested under biaxial and uniaxial conditions. This paper presents a study on the effects of biaxial stresses on the notional ultimate strength of glass. The study involved applying the theory of elasticity and finite element analysis of the *Griffith* flaw in the *micro* scale. The strain intensity at the tip of the critical flaw is used as the main criterion for defining the limit state of fracture in glass. A simple and robust relationship between the maximum principal stress and the uniaxial stress to cause failure of the same glass specimen has been developed. The relationship has been used for evaluating the strength values of both new and old annealed glass panels. The characteristic strength values determined in accordance with the test results based on 5% of exceedance are compared with provisions in the ASTM standard.

Keywords: strength of glass; biaxial effect; strain intensity; finite element

1. Introduction

The usual practice for determining the strength of glass subjected to biaxial bending is by taking the value of the maximum principal stress as if the glass was in uniaxial bending (Watchman *et al.* 2009). It is shown in this paper that the ultimate behaviour of glass depends on both the maximum and minimum (major and minor) principal stresses surrounding the tip of the critical flaw because of their complex interactions. The amount of stress that the tip of a flaw can sustain without initiating further crack growth is actually dependent on the amount of stress that co-exists in the orthogonal directions. Thus, brittle materials like glass exhibit very different strength behaviour in the uniaxial and biaxial stress states.

The objective of this paper is to present analytical work that has been undertaken to develop a simple and robust transformation relationship between the maximum and minimum principal stresses (σ_1 and σ_2) and equivalent uniaxial stress (σ_u) that is estimated to cause failure of the glazing panel (Section 3). The proposed correction relationship is illustrated with applications on real experimental data (Section 4). The corrected data of the failure stresses has been evaluated by

---

*Corresponding author, Ph.D. Student, E-mail: ilham@undip.ac.id

matching with various well known distribution relationships and by comparison with provisions in the ASTM standard.

2. Current practice for determining the strength of glass

In practice, glazing panels are typically subjected to bending when out-of-plane wind pressure is applied. Several test methods have been developed to examine the bending strength of glass. These test methods can be divided into uniaxial bending tests and biaxial bending tests. With uniaxial bending tests, specimens are supported on two ends and subject to one or two concentrated line loads causing bending in one direction (Fig. 1(a)). The advantage of this test method is that only one principal stress is developed at all locations in the glass specimen. Hence, possible influences by the other (minor) principal stress have been neglected. The uniaxial bending test with two concentrated line loads is also known as *four-point bending* test (ASTM-C158 2002, EN-1288-3 2000).

With biaxial bending tests, specimens undergo bending in two directions. Biaxial bending tests commonly used in practice are namely *ball-on-ring* tests (Oh *et al.* 2003, Shetty *et al.* 1981), *uniform pressure* tests (Beason and Morgan 1984, Calderone 2000, Dalgliesh and Taylor 1990), or *coaxial double-ring* tests (EN-1288-2 2000, EN-1288-5 2000). The schematics of the mentioned biaxial bending tests are shown in Figs. 1(b)-1(d) respectively. With specimens subject to two-way bending (i.e., biaxial stresses), the notional ultimate strength is usually taken as the maximum (major) principal stress identified at the instance of failure of the specimen. Meanwhile, contributions of the minimum (minor) principal stresses to the bending resistance of the specimen have been neglected.

It is known that the strength of glass obtained from tests is dependent on the location of the critical flaw which initiates fracture in the specimen. As the critical flaw is randomly positioned in a specimen, the ratio of the principal stresses (σ_2/σ_1) at the location of the critical flaw is variable. The effect of the value of the stress ratio on ultimate strength can be analysed by correlating the major principal stress value at failure against the stress ratio at the location of fracture initiation. However, the strength of the specimen is also controlled by the size of the critical flaw. Thus, the value of the notional ultimate strength (i.e., maximum value of principal stress at failure) for any given location can vary because of variable size of the critical flaw in the individual specimens (Nurhuda *et al.* 2010). Thus, a good correlation of the maximum principal stress at failure with the principal stress ratio could be obtained if there is an abundance of test data provided that properties of individual microcracks including its size and fractal geometry have also been controlled. This can be achieved experimentally by incorporating an artificial major flaw in the specimen or analytically by incorporating pre-determined critical flaws of an ideal geometry in the finite element model.

Well known principles based on the maximum normal stress criterion has been supported by experimental data under the conditions of plane stress state (Lebedev *et al.* 2001). However, the effects of biaxial stresses on the strength of glass is very complex and warrant further studies given that so many factors are involved in controlling real behaviour (Lebedev *et al.* 2001, Liebowitz 1968, Rodichev and Tregubov 2009, Veer *et al.* 2008). The critical (at failure) Stress Intensity value (K_I) as defined by Eq. (1) may be sensitive to the conditions of biaxial tension mainly because the effects of biaxial actions is not well represented by stresses alone. Notwithstanding, the effects of biaxial stress on the strength of glass have been acknowledged in the literature (Bao *et al.* 2005,

(a) Four point bending (4PB) test

(b) Ball on ring test

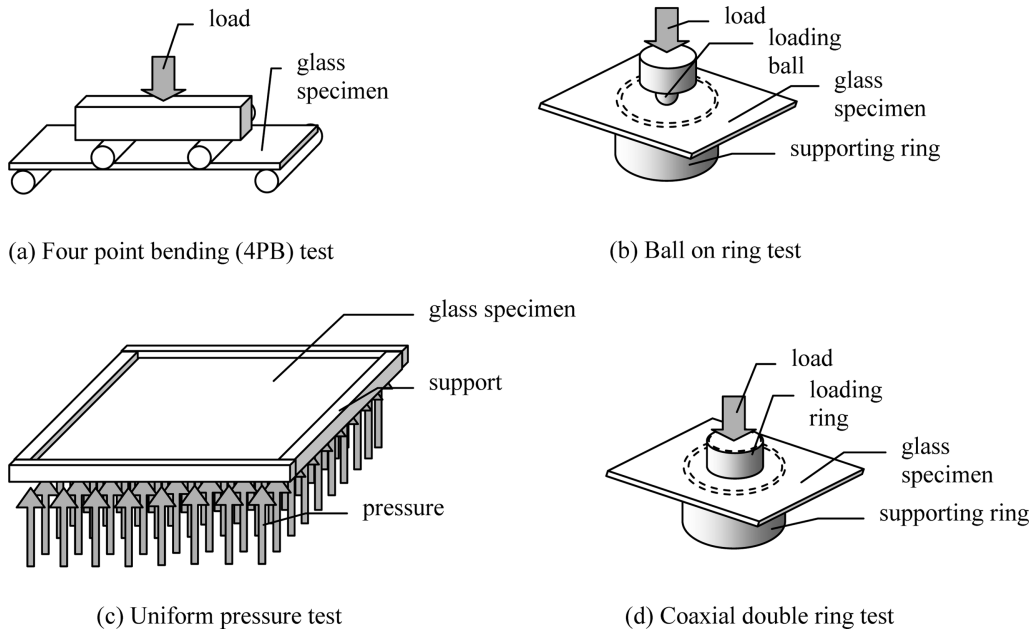(c) Uniform pressure test

(d) Coaxial double ring test

Fig. 1 Test methods for investigating bending strength of glass

Beason and Morgan 1984, Danzer *et al.* 2006, Oh *et al.* 2003, Shetty *et al.* 1981). For example, Beason (1984) formulated the effect of biaxial stress based on the probability of the orientation of the critical flaws. Beason's theory is adopted in the ASTM provision E1300 for determining the strength of glass.

$$K_I = \sigma_1 \cdot Y \cdot \sqrt{\pi \cdot a} \qquad (1)$$

where K_I is stress intensity, σ_1 is uniaxial stress applied normal to the axis of the flaw, Y is shape factor, and a is half the flaw dimension.

Whilst the orientation of the critical flaw has been considered in Beason's model, the significant of the stress parallel to the crack has not been considered. Experimental studies by Naumenko and Atkins (2006) showed the significant contribution of the tensile stress parallel to the crack in resisting crack extension. This finding confirms results of previous studies which revealed that biaxial stress ratios affect the velocity of crack propagation (Kitaoka and Mikuriya 1996). This paper is concerned with a theoretical aspect of the contribution of the principal stress which is parallel to a crack to the strength of glass (which is not well represented by the stress intensity approach).

Moreover, researchers have discovered that during loading a critical flaw grows from its initial size to the final size (Porter and Houlsby 2001, Wiederhorn *et al.* 1982). The orientation of the critical flaw as well as its shape and size are important modelling parameters which need to be considered in modelling crack growth (Liebowitz 1968, Rodichev and Tregubov 2009). It has also been suggested that critical flaws undergoing sub-critical crack growth before reaching its final size tends to propagate perpendicular to the direction of the maximum principal stress (Doremus 1994, Khan and Khraisheh 2000, Nurhuda *et al.* 2010, Yates *et al.* 2008). The orientation of the newly grown cracks may accordingly be taken as deterministic which simplifies the calculation of the

strength of the specimen. However, this latest proposition is controversial.

The following section presents an analytical investigation into the effects the minimum (minor) principal stress has upon the notional ultimate strength of glass. A simple and robust transformation relationship is then proposed to model the important influences of the principal stress ratio.

3. Proposed correction relationship

In fracture mechanics, the stress intensity in a brittle material to cause crack growth from the critical flaw leading to fracture is related to the size and shape of the flaw and the applied notional uniaxial stresses as defined by Eq. (1). However, the critical stress intensity initiating fracture has been found to be dependent on the biaxial stress condition (Bao *et al.* 2005).

In theory, a brittle material will have lost all its strength if the atoms are separated to a certain critical distance. Thus, what actually matters to the ultimate behaviour of the material is strains (which controls the separation of particles and hence affecting their inter-atomic bonding). Eq. (2) has been proposed by Bao and Steinbrech (1997) for analysing failure based on the strain intensity at the tip of the critical flaw, and is the strain analogy of Eq. (1) for defining the condition of fracture initiation from the critical flaw (Guz *et al.* 2004).

$$S_I = \varepsilon_1 \cdot Y \cdot \sqrt{\pi \cdot a} \tag{2}$$

where S_I is strain intensity, ε_1 is strain normal to the axis of the flaw, Y is shape factor, and a is half the flaw dimension.

In conditions of biaxial stresses, it is assumed that the maximum principal stress (σ_1), and strain (ε_1), is applied in the direction that is normal to the axis of the critical flaw. Eq. (3) from elementary theory of elasticity defines the relationship between the principal stresses (and strains) and the Poisson's ratio. By substituting Eq. (3) into Eq. (2), the strain intensity is expressed in terms of both principal stresses (σ_1 and σ_2) as shown by Eq. (4).

$$\varepsilon_1 = \frac{\sigma_1}{E}(1 - v \cdot \alpha) \tag{3}$$

$$S_1 = \frac{\sigma_1}{E}(1 - v \cdot \alpha) \cdot Y \cdot \sqrt{\pi \cdot a} \tag{4}$$

where v is Poisson ratio and α is the principal stress ratio (σ_2/σ_1) and E is Young's modulus.

It can be seen from Eq. (4) that a material subject to biaxial tensile stresses ($\sigma_1 > 0$; $\sigma_2 > 0$) would actually sustain a higher stress level without failure than that subject to uniaxial tensile stresses ($\sigma_1 > 0$; $\sigma_2 = 0$). To identify the equivalent uniaxial tensile stress for checking against the characteristic strength of the material, Eq. (2) and Eq. (4) are combined to give Eq. (5).

$$\frac{\sigma_U}{E} \cdot Y \cdot \sqrt{\pi \cdot a} = \frac{\sigma_1}{E}(1 - v \cdot \alpha) \cdot Y \cdot \sqrt{\pi \cdot a} \tag{5a}$$

$$\frac{\sigma_1}{\sigma_U} = \frac{1}{1 - v \cdot \alpha} \tag{5b}$$

where σ_U is failure stress in uniaxial conditions.

(a) A glass panel with a straight-through flaw of 80 μm long

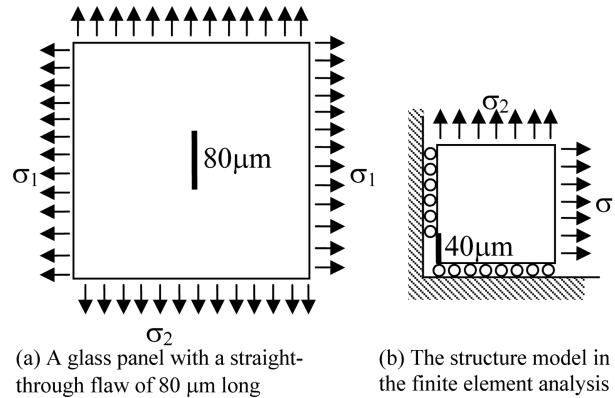(b) The structure model in the finite element analysis

Fig. 2 Structure models

It is noted that Eqs. (3)-(5) would only be valid for homogenous materials given that complex conditions surrounding the tip of the critical flaw have not been taken into account. An analytical investigation based on the use of the finite element method (FEM) was conducted to analyse stresses and strains surrounding the critical flaw. FEM analyses employing program ANSYS were used for modelling a square element of the glass pane of 1mm in dimension. This minute element which contains the critical flaw was reduced further to a quarter element (with zero shear boundaries) to minimize computational time and memory usages (Kundu 2008). The quarter element has been divided into a fine mesh of over 10,000 finite elements. The flaw being modelled was a straight-through flaw ($Y = 1$) of size 80 μm. Singular stress conditions surrounding the tip of the flaw (which has a zero radius of curvature) were simulated in the model under plane stress conditions. Uniform biaxial tensile stresses were applied from the sides of the element that were normal to the axis of the flaw (Fig. 2).

Whilst conditions for further crack growth leading to fracture is most critical at the tip of the crack where $r = 0$ (Fig. 3(a)), it is difficult to have the crack tip conditions modelled accurately by finite element analysis because of conditions of singularity. This difficulty with modelling has been circumvented by an extrapolation procedure which involves calculating the strain intensity values (S_I^*) at various points along an axis which is extended from the tip of the crack (Banks-Sills and Sherman 1986, Chan *et al.* 1970, Kundu 2008). This can be accomplished by the use of Eq. (6) and strain values (ε) obtained from FEM analyses. The strain intensity value at the crack tip (S_I) could then be obtained by linear regression and back extrapolation to the tip of the crack (where $r = 0$) as shown by Figs. 3(a) and 3(b). The strain intensity at $r = 0$ is effectively the limit of S_I^* as the value of r approaches zero (as shown by Eq. (7)).

$$S_I^* = \varepsilon \cdot \sqrt{2 \cdot \pi \cdot r} \tag{6}$$

$$S_I = \lim_{r \to 0} S_I^* \tag{7}$$

where ε is strain normal to the axis of the flaw and r is distance measured along the axis (Fig. 3(a)).

This extrapolation procedure was first verified by undertaking a control analysis in which uniform uniaxial stresses were applied to the glass pane in the direction normal to the axis of the flaw. The level of stress to cause fracture was first estimated using Eq. (1) assuming a fracture toughness (K_{IC})
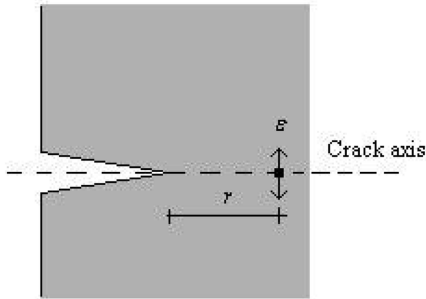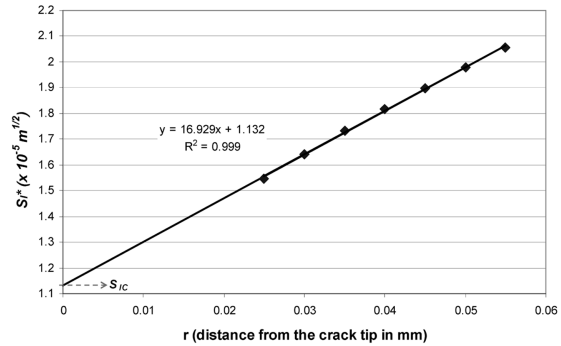
Fig. 3(a) Strain along the crack axis

Fig. 3(b) Extrapolation of the strain intensity

value of 0.78 MPa.m$^{1/2}$, $Y = 1$ (for straight-through flaw under plane stress) and flaw dimension ($2a$) of 80 μm. The uniaxial failure stress (σ_U) so calculated was 70 MPa approximately. FEM analysis of the model was then undertaken to calculate strains at various points along the axis of the flaw for this pre-determined applied uniaxial stress (70 MPa), a Young's modulus of 68500 MPa and Poisson's ratio of 0.23. Values of S_I^* that were obtained for the seven points along the axis of the flaw were linearly regressed (Fig. 3(b)) and the strain intensity at the crack tip to initiate fracture (S_I) was then estimated at 1.1323×10^{-5} m$^{1/2}$. Importantly, this value of S_I as calculated from the extrapolation procedure was highly consistent with the value that could be obtained readily by the classical method: based on dividing the fracture toughness of glass by the Young's modulus (i.e., $S_{IC} = K_{IC}/E = 1.1387 \times 10^{-5}$ m$^{1/2}$). The extrapolation procedure based on the use of Eq. (6) and Eq. (7) has therefore been verified by this control analysis.

The verified procedure was then used for analysing biaxial stress conditions in a parametric study. The objective of the study was to correlate the ratio of the two principal stresses ($\alpha = \sigma_2 / \sigma_1$) and the normalised major principal stress (σ_1/σ_U) at failure. The parametric study involved varying the value of α and Poisson's ratio (v). Failure was identified as the point when the strain intensity value reaches the critical value (S_{IC}) of 1.14×10^{-5} m$^{1/2}$. To capture this condition, stresses were applied with a gradual increase in magnitude and at least 3 pairs of results for σ_1 and S_I were identified. The limiting value of σ_1 which corresponds to $S_I = S_{IC}$ was identified by linear interpolation. Fig. 4
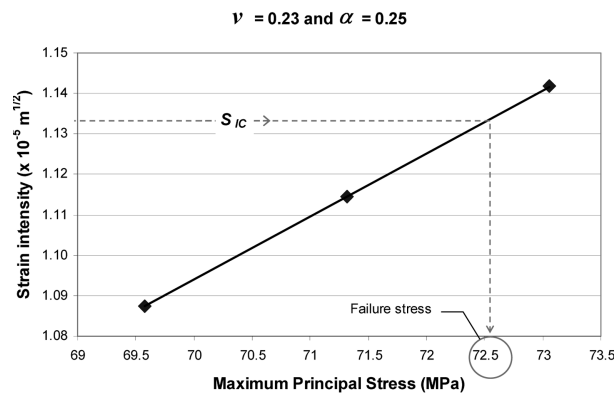

Fig. 4 Interpolation of the failure stress

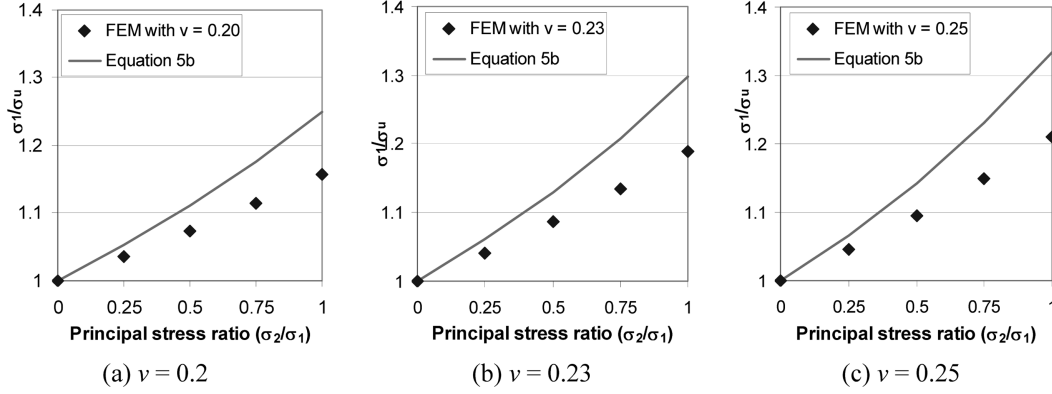(a) $v = 0.2$ (b) $v = 0.23$ (c) $v = 0.25$

Fig. 5 Comparison between FEM and Eq. (5b)

shows an example of such an interpolation in which the limiting value of σ_1 was identified as 72.5 MPa (for $v = 0.23$ and $\alpha = 0.25$). Similar analyses and interpolations were repeated for every combination of α and v in order that the limiting values of σ_1 to cause failure (i.e., 1.14×10^{-5} m$^{1/2}$) could be identified.

The parametric studies involved analysing every combination of the three Poisson's ratio values ($v = 0.20$, 0.23, 0.25) and five α values ($\alpha = 0$, 0.25, 0.5, 0.75, and 1). The corresponding values of the limiting maximum principal stress at failure are shown in Fig. 5 in the normalised form (σ_1/σ_U). For the above example of $v = 0.23$ and $\alpha = 0.25$), the value of σ_1/σ_U from finite element analysis is estimated to be at $72.5/70 = 1.03$. Significant discrepancies between results obtained from the FEM analyses and those from Eq. (5b) based on elementary theory of elasticity are clearly shown by the comparison. Interestingly, the two sets of estimates can be brought into very close agreement by applying a simple modification to Eq. (5b): incorporating factor ϕ into Eq. (8).

$$\frac{\sigma_1}{\sigma_U} = \frac{1}{(1 - v \cdot \alpha \cdot \phi)} \tag{8}$$

The factor ϕ in Eq. (8) was calibrated using the least square curve-fit technique in which the *goodness of fit* was determined by the coefficient of determination (R^2) which is defined by Eq. (9). The closer the value of R^2 to 1, the better the calibrated model matches with the referenced data. Using this approach, an optimal value of ϕ was identified to be 0.69. For all cases analysed, the value of R^2 was equal to 0.999 which is indicative of almost exact agreement.

$$R^2 = 1 - \frac{\sum_{i=1}^{N} (d_r - x)^2}{\sum_{i=1}^{N} (d_r - \overline{d}_r)^2} \tag{9}$$

where d_r is the referenced data, $\overline{d}_r$ is the average of the data, and x is the estimated value.

$$\frac{\sigma_1}{\sigma_U} = \frac{1}{(1 - 0.69 v \cdot \alpha)} \tag{10}$$

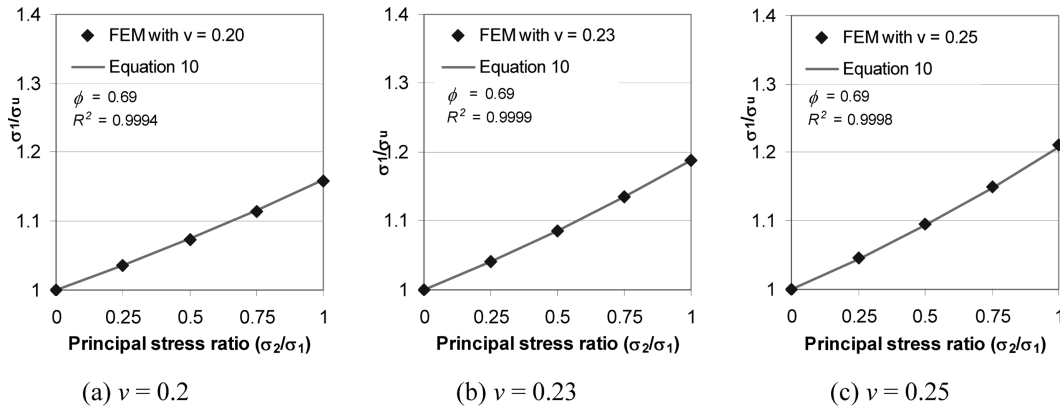(a) *v* = 0.2   (b) *v* = 0.23   (c) *v* = 0.25

Fig. 6 Comparison between FEM and Eq. (10)

Fig. 6 shows literally no discrepancies between results obtained from the FEM analyses and those from Eq. (10) which has incorporated an optimal calibrated value of $\phi = 0.69$ into the transformation expression. Furthermore, Fig. 6 shows that the strength of glass specimens subjected to biaxial stresses with the principal stress ratio of 1 can be some 20% higher than that of uniaxial stress conditions for the same critical flaw size.

4. Application of the correction relationship

Eq. (10) has been used to transform experimental data of biaxial stress values (σ_1 and σ_2) recorded at failure of the glass panels to equivalent uniaxial stress values (σ_u). There were 160 test data investigated in this research. The specimens represented by the test data were divided into 4 groups based on their size and age. The first group consisted of ninety-three specimens of new glass panels of variable size and subjected to uniform out of plane pressure. Only those specimens that did not fail by crack initiation from their edges were included in the analysis. All specimens had a length of 2000 mm and a nominal thickness of 6 mm (Table 1). The specimens were simply supported on four sides and were subject to hydrostatic pressure with three different durations of load application. Results associated with different load durations have been corrected to the reference duration of 3 seconds. Full details of the experiments can be found in Calderone (2000).

The second group of twenty new glass panel specimens of size 350 mm × 350 mm × 5 mm were subject to a point load applied at the centre point of the glass panels (each of which was supported on four sides by a wooden frame). A rubber seal was provided between the glass pane and the wooden frame to accurately simulate the conditions of contact. Loads and displacements were recorded at the centre position of the specimen. It was found from the tests that all specimens had the crack initiated from the point of contact with the load.

The third group of thirty seven specimens was from 15 year old glass panels which were simply supported on four sides and subjected to out of plane pressure (Dalgliesh and Taylor 1990). The applied pressure at failure had been converted into equivalent 60 seconds uniform pressure whilst current standards specify the strength of glass based on 3 second uniform pressure. Hence, strength transformations were required for comparing the notional strength values recorded from this test

Table 1 Summary of the specimens

Size (mm)	Thickness (mm)	Number of specimens analysed	Type of loadings	Age
2000 × 400	6	15	uniform pressures	new
2000 × 500	6	18	uniform pressures	new
2000 × 670	6	15	uniform pressures	new
2000 × 1000	6	13	uniform pressures	new
2000 × 1335	6	10	uniform pressures	new
2000 × 1600	6	11	uniform pressures	new
2000 × 2000	6	11	uniform pressures	new
350 × 350	5	20	point loads	new
1300 × 900 - 1358 × 1300	4	37	uniform pressures	old
2045 × 958	6	10	uniform pressures	old

with values specified by the standards. The conversion of strength was conducted using Eq. (11) based on the load duration theory (Brown 1972).

$$S_3 = S_{tf} \cdot \left(\frac{tf}{3}\right)^{1/n} \tag{11}$$

where *tf* is time to breakage (60 s), S_3 is equivalent constant stress causing breakage in 3 s, and *n* is 16.

The fourth group of specimens was made up of ten 35-year-old glass specimens taken from Calderone (2000). The ten specimens were of size 2045 mm × 958 mm × 6 mm and were subjected to a hydrostatic pressure. Table 1 shows summary of the specimens studied in this paper.

5. Evaluation of the corrected failure stresses

The uncorrected and corrected test results of the specimens in Section 4 were sorted in ascending order in order that the cumulative probability distribution could be calculated by Eq. (12). Three theoretical statistical distribution functions of *Weibull*, *Normal*, and *Log-Normal* were used for matching the transformed data. The goodness of fit identified for the distribution functions were evaluated and expressed in terms of the coefficient of determination (R^2) which is defined by Eq. (9). Values of the *goodness of fit* (R^2) associated with each of the distribution functions and panel size are summarized in Table 2. The cumulative probability distribution based on data that have been transformed (using Eq. (10)) is shown in Fig. 7, 8 along with data that have not been transformed.

$$CDF_i = \frac{i - 0.5}{N} \tag{12}$$

where *i* is rank of data, CDF_i is cumulative probability distribution value for the ith ranked data, *N* is number of sample.
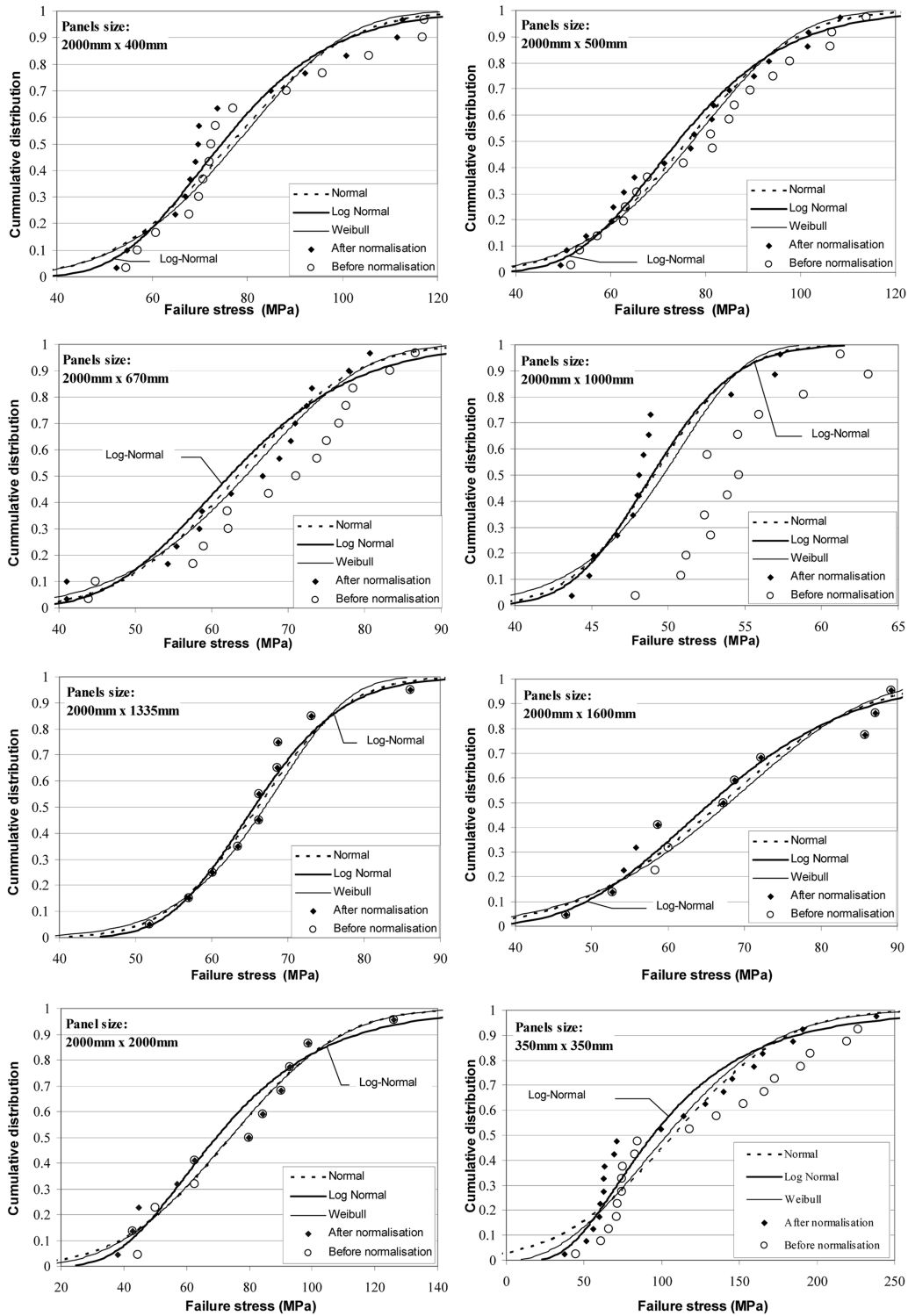
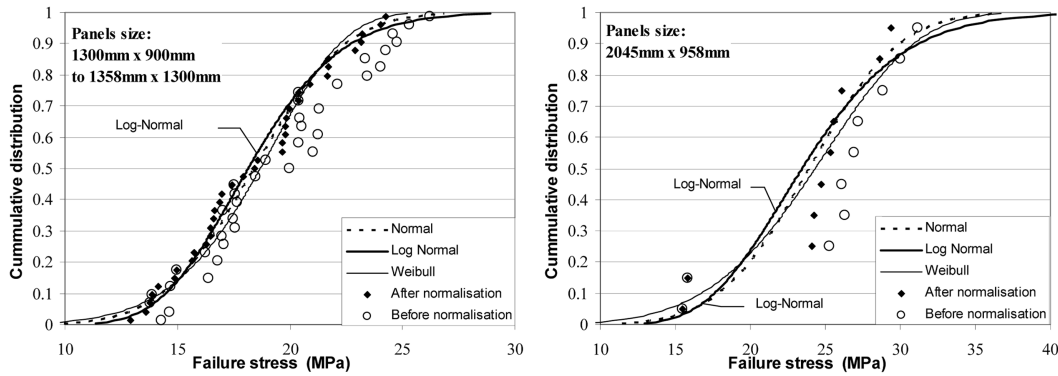Fig. 7 Cumulative probability distribution of the equivalent uniaxial failure stress of new glass specimen

Fig. 8 Cumulative probability distribution of the equivalent uniaxial failure stress of old glass specimens

It can be seen from the R^2 values listed in Table 2 that the *Log-Normal* distribution function fits with the corrected data better than the *Normal* or the *Weibull* distribution function in six out of the ten cases presented. The estimated strength of glass at low probability of failure in particular was very sensitive to the choice of the distribution function. Hence, it is important that the *Log-Normal* distribution function is used in determining the characteristic strength of the glass panels which is based on 5% of exceedance (i.e., 1 out of 20 specimens fails at a stress level lower than the characteristic strength value). The characteristic strength values evaluated in this study for 160 specimens covering both new and old glass panels are summarised in Table 3. Results from new glass panels are constrained within the range: 36 MPa-52 MPa. However, strength values obtained

Table 2 R^2 from different statistical functions

Specimen's size (mm)	R^2		
	Normal	Log-Normal	Weibull
2000 × 400 × 6	0.90	0.94	0.87
2000 × 500 × 6	0.97	0.96	0.96
2000 × 670 × 6	0.94	0.87	0.96
2000 × 1000 × 6	0.86	0.88	0.76
2000 × 1335 × 6	0.94	0.95	0.90
2000 × 1600 × 6	0.93	0.93	0.92
2000 × 2000 × 6	0.95	0.95	0.96
350 × 350 × 5	0.90	0.94	0.94
1300 × 1358 × 4	0.97	0.99	0.94
2045 × 958 × 5	0.82	0.70	0.79

Table 3 Characteristic strength values derived from the corrected test results

Specimen size (mm)	2000 × 400	2000 × 500	2000 × 670	2000 × 1000	2000 × 1335
Strength (MPa)	50	50	44	42	52
Specimen size (mm)	2000 × 1600	2000 × 2000	350 × 350	1300 × 900 (old)	2045 × 958 (old)
Strength (MPa)	45	36	39	14	16

from old glass panels have been constrained to the much narrower range: 14 MPa-16 MPa (which is about 2.5 times lower than the strength obtained from new glass panels).

Modelling size effects has been written in a separate paper (Nurhuda *et al.* 2010) and is beyond the scope of this paper. However, it is clear from Table 3 that there is a general trend of decreasing strength of the panel with increasing size. An interesting result is shown by the point load tests, which were applied to specimens of size 350 mm × 350 mm. Individual test results recorded from these tests varied very widely, from 39 MPa to 238 MPa as presented in Fig. 7. The phenomenon of high variability with the "point load" tests can be explained by the localised nature of the contact area between the load and the glass pane (where crack growth leading to fracture is initiated).

Fig. 9 shows the characteristic strength values listed in Table 3 in comparison with stipulations by the ASTM standard (ASTM-E1300 2007) based on Eq. (13) and (14) at two different levels of probability of failure. The probability of failure of 0.05 is consistent with the definition of the characteristic strength values in accordance with test results. The probability of failure of 0.008 is the basis of the allowable design strength specified by the ASTM standard.

$$\sigma = \left(\frac{P_b}{[k \cdot (d/3)^{7/n} * A]} \right)^{1/7} \qquad (13)$$

$$A = b * l \qquad (14)$$

where σ is stress, P_b is probability of breakage, d is the duration of the loading, n is 16 for annealed glass, k is a surface flaw parameter ($2.86 \times 10^{-53} \, N^{-7} \, m^{12}$), A is the surface area of the glass panel, b and l are the width and the length of the glass panel respectively.

It can be seen from Fig. 9 that the notional ultimate strength as defined by Eq. (13) with $P_b = 0.05$ is very conservative for estimating the strength of new glass specimens. With old glass specimens, the strength predictions from ASTM are slightly higher than that observed from the test results. However, the allowable design strength as defined by Eq. (13) with $P_b = 0.008$ is found to be in good agreement with strength values observed from the testing of old glass specimens.
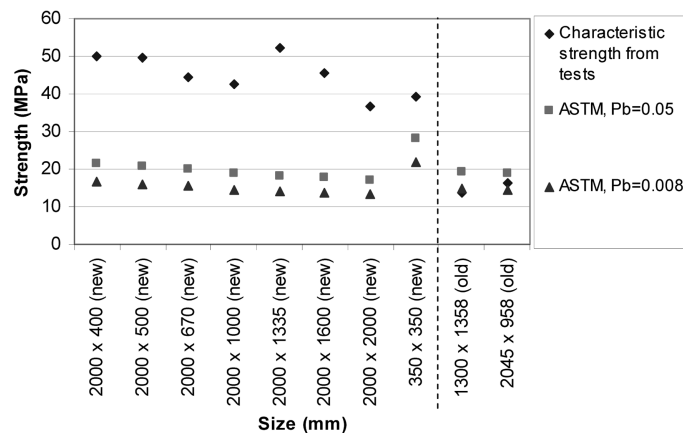

Fig. 9 Strengths of glass from different calculation methods

6. Conclusions

1. In the analysis of biaxial actions, the presented alternative approach based on the strain intensity criteria is practical and prospective for subsequent study and for more fundamental justifications.

2. A simple closed form expression based on the elementary theory of elasticity was modified by the incorporation of the ϕ factor to make allowance for the complex interactions of the orthogonal stresses without any significant loss of accuracies. This expression can be used to transform maximum principal stress values in a biaxial stress condition to equivalent uniaxial stress values to cause failure in glass panels.

3. The cumulative probability distribution of the corrected strength values was found to match reasonably well with a calibrated *Log-Normal* probabilistic distribution relationship as opposed to a *Normal* or *Weibull* distribution relationship.

4. Characteristic strength values which correspond to 5% of exceedance have been identified for glass of different dimensions, load conditions and age. Results are compared with stipulations by the ASTM standard. Strength values estimated from the ASTM standard for the same level of probability of failure are shown to be much lower than that inferred from the test results of new specimens but are in good agreement with test results of old specimens.

References

ASTM-C158 (2002), *Standard Test Method for Strength of Glass by Flexure*, ASTM International, West Conshohocken, PA.

ASTM-E1300 (2007), *Standard Practice for Determining Load Resistance of Glass in Buildings*, ASTM International, West Conshohocken, PA.

Banks-Sills, L. and Sherman, D. (1986), "Comparison of methods for calculating stress intensity factors with quarter point elements", *Int. J. Fract.*, **32**, 127-140.

Bao, Y. and Steinbrech, R.W. (1997), "Strain criterion of fracture in brittle materials", *J. Mater. Sci. Lett.*, **16**, 1533-1535.

Bao, Y.W., Li, W.H. and Qiu, Y. (2005), "Investigation in biaxial stress effect on mode I fracture resistance of brittle materials by FEM simulation and K-G-J-d relationship", *Mater. Lett.*, **59**, 439-445.

Beason, W.L. and Morgan, J.R. (1984), "Glass failure prediction model", *J. Struct. Eng.-ASCE*, **110**(2), 197-212.

Brown, W.G. (1972), *A Load Duration Theory for Glass Design*, National Research Council of Canada, Otawa.

Calderone, I. (2000), "The equivalent wind loading for window glass design", Ph.D Thesis, Monash University.

Chan, S.K., Tuba, I.S. and Wilson, W.K. (1970), "On the finite element method in linear fracture mechanics", *Eng. Fract. Mech.*, **2**, 1-17.

Dalgliesh, W.A. and Taylor, D.A. (1990), "The strength and testing of window glass", *Can. J. Civil Eng.*, **17**, 752-762.

Danzer, R., Supancic, P. and Harrer, W. (2006), "Biaxial tensile strength test for brittle rectangular plates", *J. Ceram. Soc. Jpn.*, **114**(11), 1054-1060.

Doremus, R.H. (1994), *Glass Science*, John Wiley and Sons Inc., Toronto.

EN-1288-2 (2000), *Glass in Building-Determination of the Bending Strength of Glass-Part 2: Coaxial Double Ring Test on Flat Specimens with Large Test Surface Areas*, CEN.

EN-1288-3 (2000), *Glass in Building-Determination of the Bending Strength of Glass-Part 3: Test with Specimen Supported at Two Points (four point bending)*, CEN.

EN-1288-5 (2000), *Glass in Building-Determination of the Bending Strength of Glass-Part 5: Coaxial Double Ring Test on Flat Specimens with Small Test Surface Areas*, CEN.

Guz, A.N., Dyshel, M.S. and Nazarenko, V.M. (2004), "Fracture and stability of materials and structural

members with cracks: approaches and results", *Int. Appl. Mech.*, **40**(12), 1323-1359.

Khan, S.M.A. and Khraisheh, M.K. (2000), "Analysis of mixed mode crack initiation angles under various loading conditions", *Eng. Fract. Mech.*, **67**, 397-419.

Kitaoka, S. and Mikuriya, T. (1996), "The effect of biaxial stress ratio on the propagation behaviour of mode I surface cracks by the combination of plane bending and cyclic torsion", *Int. J. Fatigue*, **18**(3), 205-211.

Kundu, T. (2008), *Fundamentals of Fracture Mechanics*, CRC Press, New York.

Lebedev, A.A., Koval'chuk, B.I., Giginjak, F.F. and Lamashevsky, V.P. (2001), *Handbook of Mechanical Properties of Structural Materials at a Complex Stress State*, (Ed. A.A. Lebedev), Begell House Inc., New York.

Liebowitz, H. (1968), *Fracture: Vol. II. Mathematical Fundamentals*, Ac Press, New York.

Naumenko, V.P. and Atkins, A.G. (2006), "Engineering assessment of ductile tearing in uniaxial and biaxial tension", *Int. J. Fatigue*, **28**, 494-503.

Nurhuda, I., Lam, N.T.K., Gad, E.F. and Calderone, I. (2010), "Estimation of strengths in large annealed glass panels", *Int. J. Solids Struct.*, **47**, 2591-2599.

Nurhuda, I., Lam, N.T.K., Dahal, R. and Gad, E.F. (2010), "Finite element analysis of the propagation of cracks in glass", *Presented at the 21th ACMSM*, December 2010, Melbourne.

Oh, S.Y., Shin, H.S. and Suh, C.M. (2003), "Evaluation of Biaxial Bending Strength in Damaged Soda Lime Glass", *Int. J. Modern Phys. B*, **17**(8 & 9), 1329-1334.

Porter, M.I. and Houlsby, G.T. (2001), "Development of crack size and limit state design methods for edge-abraded glass members", *Struct. Eng.*, **79**(8), 29-35.

Rodichev, Y. and Tregubov, N. (2009), "The challenge of quality and strength of the hardened architectural glass", *Proceedings of GPD 2009*, Tampere.

Shetty, D.K., Rosenfield, A.R., Bansal, G.K. and Duckworth, W.H. (1981), "Biaxial fracture studies of a glass-ceramic", *J. Am. Ceram. Soc.*, **64**(1), 1-4.

Veer, F.A., Louter, P.C. and Bos, F.P. (2008), "The strength of architectural glass", *Proceedings of the Conference on Architectural and Structural Application of Glass*, IOS Press, Delf.

Watchman, J.B., Cannon, W.R. and Mattewson, M.J. (2009), *Mechanical Properties of Ceramics*, John Wiley & Sons, Inc.

Wiederhorn, S.M., Freiman, S.W., JR, E.R.F. and Simmons, C.J. (1982), "Effects of water and other dielectrics on crack growth", *J. Mater. Sci.*, **17**, 3460-3478.

Yates, J.R., Zanganeh, M., Tomlinson, R.A., Brown, M.W. and Diaz Garrido, F.A. (2008), "Crack paths under mixed mode loading", *Eng. Fract. Mech.*, **75**(3-4), 319-330.